

Paso doble: A two-step Late Pleistocene range expansion in the Tyrrhenian tree frog *Hyla sarda*

1 Giada Spadavecchia¹, Andrea Chiochio^{1,2}, Roberta Bisconti^{1,*.§}, Daniele Canestrelli^{1.§}.

2 ¹Dipartimento di Scienze Ecologiche e Biologiche, Università della Tuscia. Viale dell'Università
3 s.n.c., I-01100 Viterbo, Italy.

4 ² Department of Biology, Lunds Universitet, Sölvegatan 37, 223 62 Lund, Sweden.

5

6 [§]These authors contributed equally to this work

7

8 ***Correspondence:**

9 Roberta Bisconti

10 e-mail: bisconti@unitus.it

11 **RUNNING TITLE:** Evolutionary history of *Hyla sarda*

12 **Keywords:** Bayesian phylogeography, historical demography, two-epoch model, *Hyla sarda*,
13 Tyrrhenian island.

14 **Abstract**

15 The Tyrrhenian tree frog, *Hyla sarda*, is an amphibian endemic to the Tyrrhenian islands (Western
16 Mediterranean). Previous investigations of its Pleistocene evolutionary history suggested that it
17 colonised the northern portion of its current range, through a spatial diffusion process from the
18 Sardinia island, during the last glaciation. However, southern and northern portions of the species'
19 range experienced markedly different climatic conditions during the Late Pleistocene, suggesting the
20 possibility of an unusual two-step process of demographic expansion. Here, we use Bayesian
21 phylogeographic approaches to locate the ancestral area in Sardinia and to characterise better the
22 demographic component of this expansion event. These analyses located the ancestral area for *H.*
23 *sarda* populations along the central-eastern coast of the Sardinia island, within an area previously
24 shown to host suitable bioclimatic conditions for *H. sarda* populations throughout the Late
25 Pleistocene. Historical demographic reconstructions clearly showed that a two-step process of
26 demographic growth fits well the data, with northern populations expanding later than Sardinia
27 populations. The harsher climatic conditions occurred in northern islands during the glacial epoch, as
28 compared to Sardinia, likely delayed tree frog colonisation of northern territories, and the associated
29 demographic growth.

30 **Introduction**

31 Species showing unusual phylogeographic patterns might provide unique opportunities to explore the
32 role of a wide range of ecological and evolutionary processes in shaping spatial patterns of biological
33 diversity. However, to fully exploit these opportunities, we need a thorough understanding of the
34 underlying demographic histories (e.g. Barbosa et al. 2017; Canestrelli et al. 2010). During the past
35 four decades, phylogeographic investigations of temperate species in the Western Palearctic have
36 documented widespread demographic and range contractions during glacial epochs, followed by
37 expansions during subsequent interglacials (Hewitt 2000; 2004a; 2004b; 2011a; Taberlet et al. 1998).
38 Although shared among a wide range of organisms, from all sub-regions of the Western Palearctic
39 and beyond (Hewitt 2011b), this general scenario is not devoid of exceptions. One of these remarkable
40 exceptions is represented by instances of glacial demographic and range expansion for temperate
41 species, a reverse expansion-contraction scenario initially proposed for the Tyrrhenian tree frog, *Hyla*
42 *sarda* (Bisconti et al. 2011a; 2011b), and recently used to explain phylogeographic patterns in other
43 organisms (e.g. Porretta et al. 2012; Senczuk et al. 2019).

44 The Tyrrhenian tree frog is a small, cryptically coloured amphibian, endemic to the Western
45 Mediterranean islands of Sardinia and Corsica, and the Tuscan archipelago. It is a temperate species,
46 widespread from the sea level up to 1200 meters a.s.l., although it is markedly more abundant along
47 the coastal areas (Lanza et al. 2007). *H. sarda* has primarily aquatic habits, living close to lentic
48 freshwater habitats, such as pools and temporary ponds. Previous studies of its Pleistocene
49 evolutionary history (Bisconti et al. 2011a; 2011b) showed that, contrary to what has been found in
50 most temperate species studied to date, including amphibians (Zeisset et al. 2008), this tree frog
51 likely initiated a phase of major demographic expansion in the middle of the last glaciation. This
52 event, likely promoted by a glaciation-induced increase in lowland areas during the marine regression,
53 also allowed *H. sarda* to colonise the northern island of Corsica and the Tuscan archipelago, from an
54 ancestral area in Sardinia, taking advantage of a wide and persistent land bridge connecting the
55 Sardinia to Corsica throughout the glacial epoch (Bisconti et al. 2011a; 2011b).

56 Two main points left open by previous studies were: i) the geographic location of the ancestral
57 area in northern Sardinia, and ii) the timing of the northward range expansion into Corsica and the
58 Tuscan archipelago. In fact, quantitative analyses were not conducted to attempt locating the ancestral
59 area. Most importantly, while the historical demographic reconstruction clearly showed a full-glacial
60 development of the expansion event (Bisconti et al. 2011a), paleoclimatic reconstructions for the
61 Western Mediterranean indicated substantially harsher climatic conditions in central and northern
62 Corsica than in Sardinia, during the last glaciation (Kuhlemann et al. 2008; Hughes & Woodward
63 2017; Pascucci et al. 2014). In turn, this paleoclimatic reconstruction for the last glaciation suggests

64 an intriguing scenario, whereby tree frog population expansion in Corsica and the Tuscan archipelago
65 might have been delayed, as compared to Sardinia populations, leading to a two-step expansion
66 process. A first step, promoted by the glaciation-induced widening of coastal areas in Sardinia (as
67 suggested by Bisconti et al. 2011a), would have been followed by a second step leading tree frog
68 populations to complete the northward colonisation, following post-glacial climatic amelioration in
69 northern areas.

70 Here, we explore this (revised) phylogeographic scenario, through a Bayesian phylogeographic
71 analysis, coupled with new historical demographic assessments. We carried out the demographic
72 component of the analysis separately for the source (northern Sardinia) and the recolonised (Corsica
73 and the Tuscan archipelago) populations, with the following rationale. Although they belong to the
74 same phylogeographic lineage (Bisconti et al. 2011a), their demographic history might have been
75 differently shaped by the recent paleoclimatic changes of the respective geographic ranges. If this
76 was the case, their demographic reconstructions would differ accordingly. Instead, in case they
77 actually behaved as a single demographic unit in response to such changes (following Bisconti et al.
78 2011a), the respective demographic trends would be broadly similar, as they would represent two
79 independent samples of the same demographic unit.

80

81 **Materials and methods**

82 We collected tissue samples from 81 individuals of *H. sarda*. Tree frogs were sampled by toe-
83 clipping after anaesthetization in a 0.1% solution of MS222 (3-aminobenzoic acid ethyl ester) and
84 then released at the respective collection site, while tissue samples were stored in 95% alcohol.
85 Sampling and experimental procedures were approved by the Italian Ministry of Environment
86 ‘MATTM’ (protocol #8275), and Prefecture of Corsica (#2A20180206002 and #2B20180206001).
87 Samples collected for the present study were complemented with data from northern Sardinia, Corsica
88 and the Tuscan archipelago, collected by previous studies (Bisconti et al. 2011a), allowing an overall
89 sample size of 171 individuals from 18 sampling locations (Table 1, Figure 1A, and Table S1).
90 Instead, data from central and southern Sardinia from the previous studies were not considered here,
91 as these areas were shown to be populated by distinct mitochondrial sub-lineages (Bisconti et al.
92 2011a).

93 Following a step of tissue fragmentation and digestion with proteinase K, total DNA was
94 extracted using the standard phenol-chloroform method (Sambrook et al. 1989). Two mitochondrial
95 gene fragments were amplified by polymerase chain reactions (PCRs): cytochrome b (cytb) and
96 NADH dehydrogenase subunit 1 (ND1). Primers used and PCR cycling conditions were the same
97 described in Bisconti et al. (2011a). All sequencing procedures were performed by Macrogen Inc.

98 (www.macrogen.com). The multi-purpose sequence analysis suite GeneStudio (available at
99 www.genestudio.com) was used to check the electropherograms by eye, and to generate multiple
100 sequence alignments. All sequences obtained were deposited in the GenBank database (Table S1).
101 For all downstream analyses, the two gene fragments were concatenated using DnaSp 6.11.01 (Rozas
102 et al. 2017). The models of nucleotide substitution that best fit the data (HKY for both CytB and
103 ND1) were identified by means of PartitionFinder 2.1.1 (Lanfear et al. 2016) using the Bayesian
104 information criterion (Schwarz 1987).

105 The geographic location of the ancestral area for the inferred northward expansion process
106 (Bisconti et al. 2011a), was investigated by estimating a Bayesian phylogeographic diffusion model
107 in continuous space (BP), as implemented in Beast 1.10.4 (Suchard et al. 2018). The analysis was run
108 using clock models and substitution models unlinked across all partitions. A Bayesian skyline was
109 used as coalescent prior, and the strict molecular clock was enforced, as it is generally a good
110 approximation for analyses at the intrapopulation level (Yang 2006) and because, by simplifying the
111 coalescent model, it helps analyses to converge (Heled 2010). The substitution rate was set to $1.37 \times$
112 10^{-8} , as estimated for *H. sarda* by the previous study (Bisconti et al. 2011a). After some exploratory
113 runs, the final analyses were run for 100 million generations, sampled every 1000th generation, using
114 a relaxed random walk diffusion model (RRWs) with Cauchy distribution (Lemey et al. 2009).
115 Convergence among runs, effective sample size (ESS) values, and the appropriate burn-in were
116 evaluated using the software Tracer 1.7.1 (Rambaut et al. 2018). Finally, we visualised the ancestral
117 area, and its changes through time, using the Time Slicer function implemented in Spread 1.0.7
118 (Bielejec et al. 2011), which estimate Highest Posterior Density (HPD) regions for the parameter of
119 interest, based on the full tree forest.

120 Historical demographic trends were estimated through the Bayesian skyline plot (BSP) model
121 implemented in Beast. These analyses were performed using the same settings as above, ten piecewise
122 constant intervals, and a uniform prior distribution for the population size parameter. Since
123 preliminary BSP analyses suggested demographic growth following a phase of constant population
124 size, for both Sardinia and Corsica populations, we estimated the transition time between these two
125 demographic ‘epochs’ (i.e. an epoch of constant population size followed by an epoch of population
126 growth) by means of a Two-Epoch analysis in Beast (Crandall et al. 2012). For this analysis, custom
127 *.xml* files were prepared following suggestions provided by Crandall et al. (2012). Preliminary
128 analyses were run using both an exponential and a logistic model population growth. Estimates of the
129 transition time did not differ appreciably with the two models. However, the logistic model yielded
130 comparatively inferior performance statistics and is not reported here (available upon request). These

131 analyses were run for 100 million generations, sampled every 1000th generation. All the analyses with
132 Beast were run twice and then combined to generate the final results, using LogCombiner 1.10.4.

133

134 **Results**

135 We obtained concatenated sequences 1226 bp long for all the individuals analysed, leading to a final
136 alignment including 171 individuals (81 from this study, 90 from Bisconti et al. 2011a). Sequences
137 represented uninterrupted open reading frames, with no gaps or premature stop codons, indicating
138 they are functional mitochondrial DNA copies. All the analyses carried out with BEAST converged
139 to a stationary distribution, with high effective sample size values (>200) for all the parameters of
140 interest.

141 The Bayesian phylogeographic analysis identified the ancestral area of *H. sarda* populations
142 along a small stretch of the middle eastern coastal region in Sardinia (Figure 1B). According to this
143 analysis, the species remained in this area until the last glacial epoch, when it started spreading in
144 Sardinia and then to the north, toward the Corsica island and the Tuscan archipelago (see Video S1).

145 The historical demographic reconstructions carried out by means of Bayesian skyline plot
146 analyses are shown in Figure 2A. Both for populations in Sardinia and for populations in Corsica and
147 the Tuscan Archipelago, these analyses identified an initial phase of demographic stasis, followed by
148 marked population growth. However, the timeline of the inferred demographic trends was markedly
149 different. In Sardinia, the time of the most recent common ancestor (TMRCA) was dated at 129
150 thousand years ago (kya; 95%HPD: 71 – 216 kya), whereas the transition time between the two
151 demographic epochs (i.e. constant vs growth; see Figure 2B) was estimated to have occurred 58 kya
152 (95%HPD: 40 – 79 kya). Instead, in Corsica and the Tuscan Archipelago, the TMRCA was estimated
153 at 59 kya (95%HPD: 24 – 119 kya), while the transition time to the expansion epoch was dated at 34
154 kya (95%HPD: 3 – 63 kya).

155

156 **Discussions**

157 The previous phylogeographic investigation suggested that glaciation-induced widening of coastal
158 plains might have promoted a demographic and range expansion of the Tyrrhenian tree frog, during
159 the last glaciation (Bisconti et al. 2011a). On the other hand, fine-scale paleoenvironmental
160 reconstructions for the Late Pleistocene of the Tyrrhenian islands, support this scenario for the
161 Sardinia island, but not for Corsica and the other northern islands. Here, the glacial climate was
162 harsher and coastal widening was limited, compared to Sardinia (Thiede 1978; Kuhlemann et al. 2005
163 and 2008; Forzoni et al. 2015). Our Bayesian analyses of the recent evolutionary history of *H. sarda*
164 populations allowed us to reconcile these phylogeographic and paleoenvironmental perspectives and

165 suggests an intriguing new scenario for the persistence of temperate species in the Mediterranean
166 region, over glacial-interglacial cycles.

167 Our results support previous inference suggesting that *H. sarda* (re) colonised its entire range
168 during a Late Pleistocene expansion. However, they also suggest that this major expansion phase did
169 not occur as a single demographic event, but most probably through two sequential – albeit tightly
170 linked - expansion steps. The first step allowed *H. sarda* to (re) colonise the rest of the Sardinia island
171 during the last glaciation, and to expand into the extensive coastal plain opened by the glaciation-
172 induced sea-level drop north of this island. The second step, which most probably initiated close in
173 time to the end of the last glacial maximum, allowed the species to expand northward from northern
174 Sardinia, and to colonise the entire island of Corsica and the Tuscan archipelago.

175 The source area of the Late Pleistocene expansion of *H. sarda* populations was identified in a
176 narrow coastal region in north-east Sardinia (Figure 1B). During the last glaciation, the widening of
177 the coastal lowland adjoining this area was conspicuous (see Figure 1B), and it progressively gained
178 a direct connection with the vast lowland which gradually connected northern Sardinia with southern
179 Corsica. Likewise, previously estimated species distribution models (Bisconti et al. 2011a) indicated
180 high bioclimatic suitability of this area for *H. sarda*, under both current and glacial bioclimatic
181 scenarios. Hence, phylogeographic and paleoclimatic data converge in identifying this area as a
182 suitable candidate ancestral area, and source area for the subsequent demographic expansion.

183 In line with previous historical demographic reconstructions carried out at the level of the entire
184 species' range (Bisconti et al. 2011a), our Bayesian skyline plot analysis of Sardinian populations
185 suggested that the expansion event initiated in the middle of the Late Pleistocene (58 kya). To some
186 extent, this time estimate might be an overestimate, owing to the time-dependency of the molecular
187 clock (Ho et al. 2015), and the application of a molecular clock rate calibrated using the Messinian
188 salinity crisis (i.e. 5.3 million years ago). Yet this time estimate matches considerably well with a
189 phase of major sea-level drop (occurring about 65 kya; Spratt & Lisiecki, 2016), and a consequent
190 widening of coastal habitats. Most importantly, however, the estimated region of 95% highest
191 posterior probability density for this event (40 – 79 kya), rule out the possibility of a post-glacial, or
192 even a late-glacial, initiation of the demographic expansion in Sardinia. Thus, phylogeographic and
193 paleoclimatic data converge in identifying the middle of the Late Pleistocene as the most likely time-
194 frame for the expansion event in Sardinia.

195 In Corsica and the Tuscan archipelago, however, the expansion event occurred later. For these
196 populations, the inferred TMRCA is significantly more recent than for Sardinian populations, and
197 closely matches the transition time between the two demographic epochs in Sardinia (median
198 estimates: 59 vs 58 kya, respectively). Importantly, although surrounded by a non-negligible

199 uncertainty (95%HPD: 24 – 119 kya), this event appears unlikely to have followed the last glacial
200 maximum (LGM; ~23 kya; Kuhlemann et al. 2008). Instead, the same cannot be said for the
201 expansion event. Since the TMRCA, a phase of demographic stability lasting about 25 kya preceded
202 the demographic expansion. Although the median estimate for the transition time between these two
203 epochs (34 kya) precedes the LGM, the 95% highest posterior density region for this event (3 – 63
204 kya; see also Figure 2B) largely incorporates the LGM and subsequent post-glacial times. Moreover,
205 since this is the most recent event inferred from our data, we can expect it to be most affected by the
206 time-dependency of the molecular clock, and the consequent inflation of recent time estimates (see
207 Membrebe et al. 2019 for an estimate of the effect size in a case where both root calibration and dated
208 tips were available). Lastly, when also considering the particularly harsh climate at the LGM in
209 Corsica, due to polar air incursions (Kuhlemann et al. 2008), and the abrupt transition to post-glacial
210 environmental conditions in this area (Kuhlemann et al. 2005 and 2008; Forzoni et al. 2015), a
211 scenario considering a peri-glacial initiation and post-glacial development of the range expansion in
212 Corsica appears the most plausible for a thermophilic species, as is *H. sarda*.

213

214 **Conclusions**

215 Our study allowed to improve previous estimates of the evolutionary history of the Tyrrhenian tree
216 frog *H. sarda*, by 1) locating the source area of its major range expansion in the Late Pleistocene, and
217 2) identifying a previously undetected component of the associated demographic trends. On the one
218 hand, the inferred two-step expansion model is unprecedented for temperate species in the
219 Mediterranean region and will deserve further evaluation in other temperate species. These studies
220 should be focused on species both from insular geographic settings and from mainland areas close to
221 coastal regions which have been particularly affected by glacial widenings of lowland habitats (e.g.
222 the Adriatic Sea, central Mediterranean). On the other hand, by providing unusual resolution to the
223 temporal and geographic components of its recent evolutionary history, our results place *H. sarda* in
224 an excellent position to become a prominent case for the study of the genomic and phenotypic legacy
225 of Late Pleistocene range dynamics of island species.

226 Finally, although previous studies showed no significant discrepancy between nuclear and
227 mtDNA data (Bisconti et al. 2011a), results from the present study should be confirmed with in-depth
228 analyses of the nuclear genome. Whole-genome sequencing will be useful to precisely calibrate the
229 molecular clock, to confirm the demographic dynamics that emerged in the present study, and to
230 investigate the evolutionary implications of these dynamics.

231 **Acknowledgements**

232 We are grateful to Alessandro Carlini, Giacomo Grignani, Lorenzo Latini, Anita Liparoto, Armando
233 Macali, for assistance with sampling and the experimental procedures. The research was supported
234 by a grant from the Italian Ministry of Education, University and Research (PRIN project
235 2017KLZ3MA).

236 **Author contributions**

237 R.B. and D.C. designed the study; G.S., A.C., R.B. and D.C. performed research; G.S. and D.C.
238 analyzed data; G.S., R.B. and D.C. wrote the paper; G.S., A.C., R.B. and D.C. discussed and approved
239 the final version of the manuscript.

240 **Conflict of Interest**

241 The authors declare that the research was conducted in the absence of any commercial or financial
242 relationships that could be construed as a potential conflict of interest.

243 **References**

- 244 **Barbosa S, Paupério J, Herman JS, Ferreira CM, Pita R, Vale-Gonçalves HM, & Mira A. 2017.**
245 Endemic species may have complex histories: Within-refugium phylogeography of an endangered
246 Iberian vole. *Molecular ecology*, 26(3), 951-967.
- 247 **Bielejec F, Rambaut A, Suchard MA, Lemey P. 2011.** SPREAD: spatial phylogenetic
248 reconstruction of evolutionary dynamics. *Bioinformatics*, 27(20), 2910-2912.
- 249 **Bisconti R, Canestrelli D, Colangelo P, Nascetti G. 2011a.** Multiple lines of evidence for
250 demographic and range expansion of a temperate species (*Hyla sarda*) during the last glaciation.
251 *Molecular Ecology*, 20(24), 5313-5327.
- 252 **Bisconti R, Canestrelli D, Nascetti G. 2011b.** Genetic diversity and evolutionary history of the
253 Tyrrhenian treefrog *Hyla sarda* (Anura: Hylidae): adding pieces to the puzzle of Corsica–Sardinia
254 biota. *Biological Journal of the Linnean Society*, 103(1), 159-167.
- 255 **Canestrelli D, Aloise G, Cecchetti S, Nascetti G. 2010.** Birth of a hotspot of intraspecific genetic
256 diversity: notes from the underground. *Molecular Ecology*, 19(24), 5432-5451.
- 257 **Crandall ED, Sbrocco EJ, DeBoer TS, Barber PH, Carpenter KE. 2012.** Expansion dating:
258 calibrating molecular clocks in marine species from expansions onto the Sunda Shelf following the
259 Last Glacial Maximum. *Molecular Biology and Evolution*, 29(2), 707-719.
- 260 **Forzoni A, Storms JEA, Reimann T, Moreau J, Jouet G. 2015.** Non-linear response of the Golo
261 River system, Corsica, France, to Late Quaternary climatic and sea level variations. *Quaternary
262 Science Reviews*, 121, 11-27.
- 263 **Heled J. 2010.** Extended Bayesian skyline plot tutorial. Available from [http://beast-
264 mcmc.googlecode.com](http://beast-mcmc.googlecode.com)
- 265 **Hewitt G. 2000.** The genetic legacy of the Quaternary ice ages. *Nature*, 405(6789), 907.
- 266 **Hewitt G. 2004a.** Genetic consequences of climatic oscillations in the Quaternary. Philosophical
267 Transactions of the Royal Society of London. *Series B: Biological Sciences*, 359(1442), 183-195.
- 268 **Hewitt G. 2004b.** The structure of biodiversity—insights from molecular phylogeography. *Frontiers
269 in zoology*, 1(1), 4.
- 270 **Hewitt G. 2011a.** Mediterranean Peninsulas—the evolution of hotspots. In: Biodiversity Hotspots
271 (eds Zachos FE and Habel JC), pp. 123–148. Springer, Amsterdam.
- 272 **Hewitt G. 2011b.** Quaternary phylogeography: the roots to hybrid zones. *Genetica*, 139, 617–638.
- 273 **Ho SY, Duchêne S, Molak M, Shapiro B. 2015.** Time-dependent estimates of molecular
274 evolutionary rates: evidence and causes. *Mol Ecol*. 2424:6007 – 6012. doi: 10.1111/mec.13450
- 275 **Hughes PD, Woodward JC. 2017.** Quaternary Glaciation in the Mediterranean Mountains.
276 Geological Society, London, Special Publications, 433, 1–23.
- 277 **Kuhlemann J, Frisch W, Székely B, Dunkl I, Danišik M, Krumrei I. 2005.** Würmian maximum
278 glaciation in Corsica. *Austrian Journal of Earth Sciences*, 97, 68-81.

- 279 **Kuhlemann J, Rohling EJ, Krumrei I, Kubik P, Ivy-Ochs S, Kucera M. 2008.** Regional synthesis
280 of Mediterranean atmospheric circulation during the last glacial maximum. *Science*, 321, 1338–1340.
- 281 **Lanza B, Andreone F, Bologna MA, Corti C, Razzetti E. 2007.** Fauna d'Italia Amphibia.
282 Calderini, Bologna.
- 283 **Lanfear R, Frandsen PB, Wright AM, Senfeld T, Calcott B. 2016.** PartitionFinder 2: new methods
284 for selecting partitioned models of evolution for molecular and morphological phylogenetic analyses.
285 *Molecular biology and evolution*.
- 286 **Lemey P, Rambaut A, Drummond AJ, Suchard MA. 2009.** Bayesian phylogeography finds its
287 roots. *PLoS computational biology*, 5(9), e1000520.
- 288 **Membrebe JV, Suchard MA, Rambaut A, Baele G, Lemey P. 2019.** Bayesian inference of
289 evolutionary histories under time-dependent substitution rates. *Molecular biology and
290 evolution*, 36(8), 1793-1803.
- 291 **Pascucci V, Sechi D, Andreucci S. 2014.** Middle pleistocene to holocene coastal evolution of NW
292 sardinia (Mediterranean Sea, Italy). *Quaternary International*, 328, 3-20.
- 293 **Porretta D, Mastrantonio V, Bellini R, Somboon P, Urbanelli S. 2012.** Glacial history of a modern
294 invader: phylogeography and species distribution modelling of the Asian tiger mosquito *Aedes
295 albopictus*. *PloS one*, 7(9).
- 296 **Rambaut A, Drummond AJ, Xie D, Baele G, Suchard MA. 2018.** Posterior summarization in
297 Bayesian phylogenetics using Tracer 1.7. *Systematic biology*, 67(5), 901-904.
- 298 **Rozas J, Ferrer-Mata A, Sánchez-DelBarrio JC, Guirao-Rico S, Librado P, Ramos-Onsins SE,
299 Sánchez-Gracia A. 2017.** DnaSP 6: DNA sequence polymorphism analysis of large data sets.
300 *Molecular Biology and Evolution*, 34(12), 3299-3302.
- 301 **Sambrook J, Fritsch EF, Maniatis T. 1989.** Molecular cloning: a laboratory manual (Ed. 2). Cold
302 spring harbor laboratory press.
- 303 **Schwarz G. 1987.** Estimating the dimension of a model. *The annals of statistics*, 6(2), 461-464.
- 304 **Senczuk G, Harris DJ, Castiglia R, Litsi Mizan V, Colangelo P, Canestrelli D, Salvi D. 2019.**
305 Evolutionary and demographic correlates of Pleistocene coastline changes in the Sicilian wall lizard
306 *Podarcis wagleriana*. *Journal of Biogeography*, 46(1), 224-237.
- 307 **Spratt RM, Lisiecki LE. 2016.** A Late Pleistocene sea level stack. *Climate of the Past*, 12(4), 1079-
308 1092.
- 309 **Suchard MA, Lemey P, Baele G, Ayres DL, Drummond AJ, Rambaut A. 2018.** Bayesian
310 phylogenetic and phylodynamic data integration using BEAST 1.10. *Virus Evolution*, 4(1), vey016.
- 311 **Taberlet P, Fumagalli L, Wust-Saucy AG, Cosson JF. 1998.** Comparative phylogeography and
312 postglacial colonization routes in Europe. *Molecular ecology*, 7(4), 453-464.
- 313 **Thiede J. 1978.** A glacial Mediterranean. *Nature*, 276, 680–683.
- 314 **Yang Z:** Computational Molecular Evolution. Oxford University Press 2006, Oxford, UK

315 **Zeisset I, Beebee TJC. 2008.** Amphibian phylogeography: a model for understanding historical
316 aspects of species distributions. *Heredity*, *101*(2), 109-119.

317 **SUPPORTING INFORMATION**

318 Additional Supporting Information may be found in the online version of this article at the
319 publisher's web-site:

320 **Table S1.** Complete dataset generated and used in this study.

321 **Video S1.** Animation of the spatial diffusion through time of *Hyla sarda* in virtual globe software
322 (GoogleEarth).

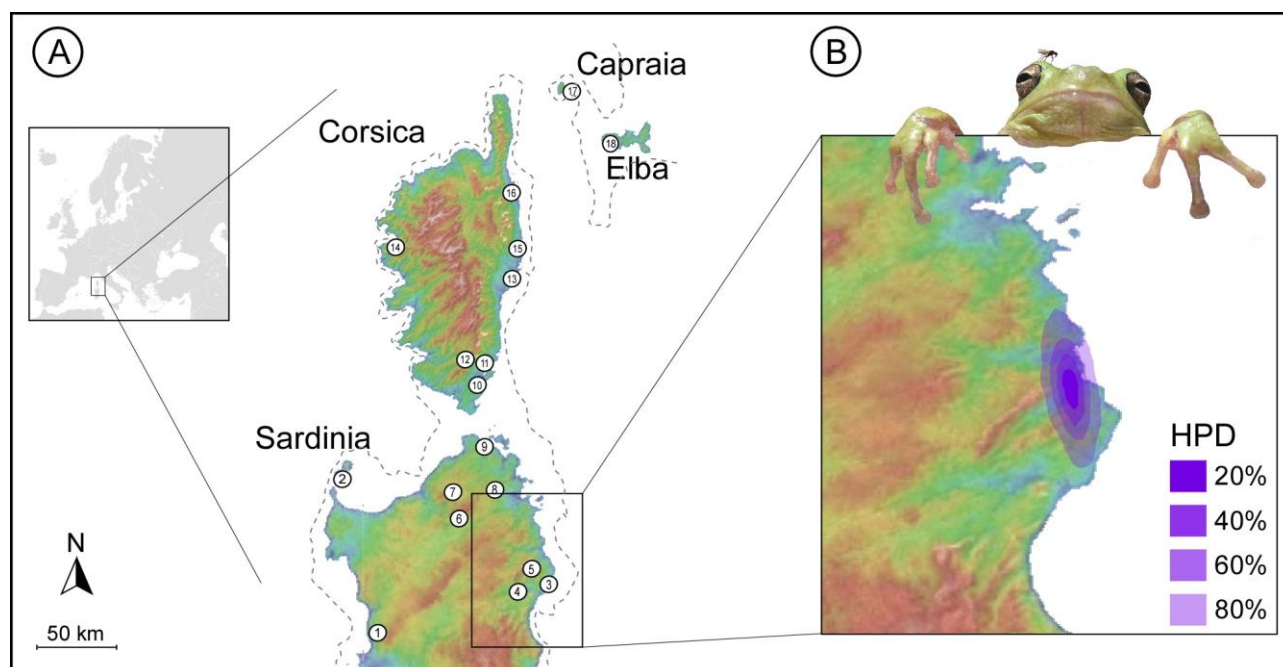
323 **Table 1.** Sampling location and sample size (n) for the 18 populations of *Hyla sarda* analysed for
324 the present study.

Island		Locations	n	Latitude N	Longitude E
Sardinia	1	Monteferro	14	40°12'	08°35'
	2	Asinara	2	41°03'	08°14'
	3	Cala Ginepro	8	40°26'	09°47'
	4	Siniscola	25	40°34'	09°46'
	5	Posada	6	40°38'	09°45'
	6	Vallicciola	5	40°51'	09°09'
	7	Luogosanto	9	41°03'	09°12'
	8	Stazzo Pulcheddu	6	41°09'	09°21'
	9	Porto Pollo	9	41°11'	09°19'
Corsica	10	Etang de Canettu	6	41°25'	09°13'
	11	T10	10	41°26'	09°12'
	12	L'Ospedale	12	41°39'	09°11'
	13	Aleria	11	42°06'	09°31'
	14	Curzo	9	42°19'	08°40'
	15	San Giuliano	7	42°16'	09°31'
	16	Biguglia	3	42°38'	09°26'
Capraia	17	Capraia	5	43°02'	09°50'
Elba	18	Elba	25	42°47'	10°15'

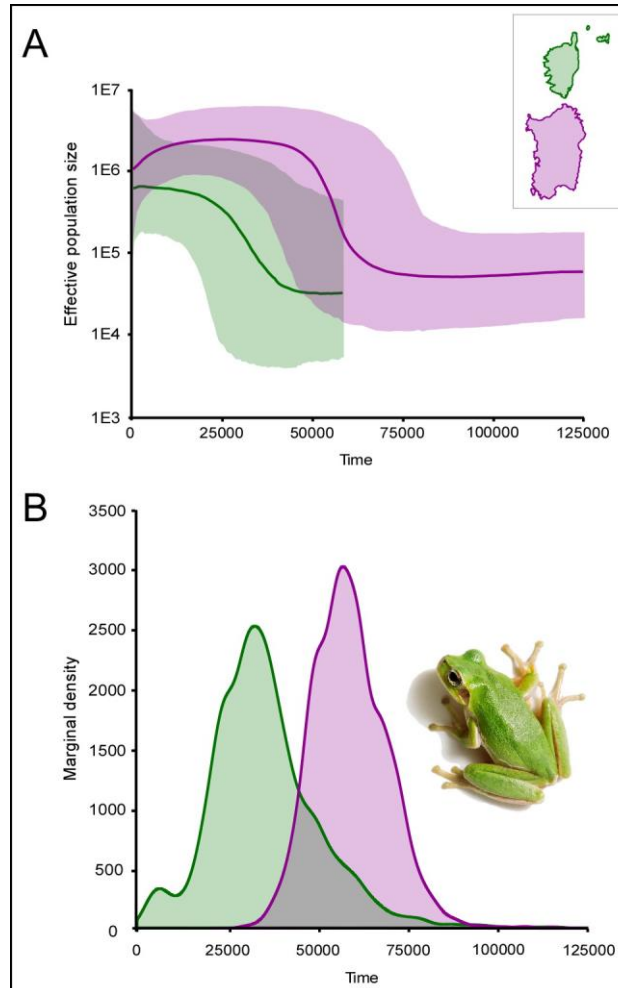
325

326 **Figure 1.** A) Study area and geographic location of the 18 sampled populations of *H. sarda*. The
327 dashed line shows the approximate location of the coastline during the last glacial maximum (Thiede,
328 1978). B) Highest posterior density (HPD) regions of the ancestral area of *H. sarda*, based on a
329 Bayesian phylogeographical analysis carried out in Beast.

330



331 **Figure 2.** Historical demographic reconstructions for the Sardinian populations (purple), and the
332 Corsica and Tuscan archipelago populations (green). A) Bayesian skyline plots showing the effective
333 population size change through time. Median estimates and 95% highest posterior density regions are
334 shown (continuous line and shaded areas, respectively). B) Marginal posterior probability
335 distributions for the transition time to exponential growth from the two-epoch models.



336